COMBUSTION SYNTHESIZED Al^{+3} SUBSTITUTED $CoFe_2O_4$ FOR STRUCTURAL AND DIELECTRIC STUDIES

Nandakumar V[1], Roopadevi[2], Khaleel Ahmed[3], Asiya Parveez[4], Sindhu S[5*]

[1] Department of Physics, Govt. First Grade College for Women, Holenarasipur-573211, Karnataka, India.

[2] Department of Physics, Govt. College (Autonomous), Mandya-571401, Karnataka, India.

[3] Department of Physics, Govt. Science College (Autonomous), Hassan-573201, Karnataka, India.

[4] Department of Physics, Govt. Science College, Chitradurga-577501, Karnataka, India.

[5] Department of Applied Sciences, Guru Nanak Dev Engineering College, Bidar-585403, Karnataka, India.

Corresponding Author: Sindhu S, sindhuprasadj24@gmail.com

Abstract:

This article presents the structural and dielectric studies of trivalent metal ion (Al^{+3}) doped cobalt ferrite. Trivalent metal ion (Al^{+3}) was substituted in pure Cobalt ferrite ($CoFe_2O_4$) samples with the basic composition $CoAl_xFe_{2-x}O_4$ (here, x= 0.0, 0.1, 0.15, 0.2 and 0.25), were synthesized by auto-combustion method using the precursors such as nitrates and citrate. Synthesized samples were sintered at 950^0C and investigated for various properties. Phase of the synthesized samples were probed by X-ray diffraction (XRD) studies. Peaks observed in the XRD spectrum confirms the single phase spinel cubic structure for the Al^{+3} ion substituted $CoFe_2O_4$. Using FESEM, surface morphology of the samples has been investigated. Frequency dependent dielectric properties were studied using HIOKI make LCR meter model 3520-50 from 100Hz to 5 MHz

Keywords: Combustion; Dielectric; Frequency; Peaks; Precursors.

DOI Number: 10.48047/nq.2021.19.11.NQ21252 **NeuroQuantology 2021; 19(11): 501-506**

1. Introduction

Mostly used ferrites in the ferrite family are spinel ferrites. Nano structured soft spinel ferrites have attracted great interest due to their excellent physio-chemical properties such as , low toxicity and their magnetism as well as, because of their highly tunable properties, like its dielectric, magnetic properties, which can be easily modified just adopting various preparation techniques and various factors such as the type of organic fuel used for the synthesis, P_H of the redox solution, composition of the metal ions, crystal structure, types of additives and sintering temperature etc [1-3]. These nano-structured magnetic oxides are currently considered among the widely successful magnetic nanoparticles (MNPs) that can be extensively used for various technological and in medical applications such as electrochemical sensor applications, in storage medium, contrast enhancement in magnetic resonance imaging, suspension systems using magnetic fluids, targeted drug delivery and in many more technological devices and applications. [4-5].

Spinel magnetic oxide materials, mainly consists of Fe_2O_3 and have spinel (MFe_2O_4) cubic structure, here M represents to a divalent metal ion(s). These samples, which are ferri-magnetic in nature exhibit magnetic hysteresis (M-H curve) and at the same time exhibit spontaneous magnetization. Various properties of magnetic spinel is because of distribution of metal ions among the available

voids such as tetrahedral (A) and octahedral (B) sites [5]. For any materials of interest, its properties are highly dependent on preparation technique selected, type of synthesis environment such as in inert or in open air atmosphere, type of organic fuel used, sintering time and temperature, etc.

In case of inverse spinel structure half of the trivalent metal ions occupy tetrahedral (A-sites) and half in octahedral (B-sites), the remaining cations being randomly distributed among the B-sites. Inverse spinel ferrites are represented by the formula $(Me^{+3})_A [M^{+2}Me^{+3}]_BO_4$. Among the spinel ferrite, cobalt ferrite, $CoFe_2O_4$ (CFO), is a special type as it exhibits multiferroic properties. CFO exhibiting excellent magnetic properties, high electrical resistivity, significant hardness, chemical stability, etc. ensures potential applications in high frequency transformers, magnetic storage devices, drug delivery systems, waste water treatment, sensors [6-9].

$CoFe_2O_4$ crystallizes in a cubic inverse spinel structure. In $CoFe_2O_4$, while **Co** ions occupy the octahedral site, **Fe** ions are equally distributed in tetrahedral and octahedral sites. Generally, $CoFe_2O_4$ can be written as $(Co_{1-x}Fe_x)$ $[Co_xFe_{2-x}]$ O_4, where parentheses indicate cation site of tetrahedral coordination, square brackets indicate octahedral coordination and x indicates the degree of inversion defined as a fraction of A-sites occupied by **Fe**. Cation distribution in the respective sites are responsible for the magnetic and electrical properties displayed by ferrites. When dopants are added to control the size or morphology of the nanoparticles, the distribution of cations is disturbed. Any alteration caused by dopants in any or both the sites tends to modify their magnetic and electrical properties finally resulting in modified material behavior [10-11].

In our present study, samples of Al^{+3} ions substituted cobalt ferrite with the basic composition $CoAl_xFe_{2-x}O_4$ (here x= 0.0, 0.1, 0.15, 0.2 and 0.25) were prepared using nitrate-citrate auto-combustion method. This method is a self-propagating thermally-induced reaction of a gel, obtained from aqueous solutions containing metallic nitrates which acts as oxidizer and an organic fuel. Stoichiometric proportions between fuel and metallic nitrates are calculated according to the valencies of the reacting elements so as to provide the relation of oxidizer/fuel equal to one [12]. Here, metallic nitrates are preferred as starting materials which are also known as precursors, because of their water-soluble nature, have low ignition temperatures and are easy to prepare.

2. Materials and methods

Nano-powders of trivalent metal ion (Al^{+3}) substituted $CoFe_2O_4$ ferrite samples of basic chemical composition $CoAl_xFe_{2-x}O_4$ (here, x= 0.0, 0.1, 0.15, 0.2 and 0.25) were prepared using auto-combustion method. Precursors for starting the materials synthesis using the combustion method are Ferric Nitrate ($Fe(NO_3)_2.9H_2O$), Cobalt Nitrate ($Co(NO_3)_2.6H_2O$) Aluminum Nitrate ($Al(NO_3)_3.9H_2O$) and Citric acid ($C_6H_8O_7.H_2O$), all chemicals are of AR Grade with purity more than 99%. Aqueous solutions of metallic nitrates and Citric acid, which is here taken as organic fuel needed for auto-combustion reaction and are taken as per the stoichiometry. Equi-molar citric acid was added into the aqueous solution of metallic nitrates. Aqueous solution containing redox mixture was taken in a silica crucible and is allowed in to a muffle furnace, which was already pre-heated to a temperature of 500^0C. Redox mixture finally yields porous and fluffy voluminous ferrite powder. Obtained fluffy material was ground to get ferrite powders. As-burnt ash was sintered at 950^0C for 4 hours to get better crystallization and homogeneous cation distribution in the proposed spinel and finally ground to get proposed ferrite nano-powders.

Phase confirmation of the proposed samples were investigated using X-ray diffraction (XRD) studies using Bruker AXS D8 Advance X-ray diffractometer (using Cu-K_α radiation, λ=1.5406 Å), a working voltage of 40kV at 40mA of current. Diffraction data were collected in the 2θ range 10-70^0. Morphology of the sintered samples has been investigated using Field Emission Scanning Electron Microscope (JEOL Model 7610FPLUS). Parallel capacitance, C_p and dissipation factor, tanδ as a function of frequency in the range 100 Hz-5

MHz were measured using a precision LCR meter. Real and imaginary parts of dielectric permitivity (ε' and ε'') dielectric permitivity (ε') and (ε'') were computed using the formulae [13],

$$\varepsilon' = Ct/\varepsilon_0 A \quad (1)$$

$$\varepsilon'' = \varepsilon' \tan \delta \quad (2)$$

Where, t is the thickness and A, the area of the pellet.

The ac conductivity, σ_{ac} was determined from the dielectric loss factor using a relation

$$\sigma_{ac} = \omega \varepsilon_0 \varepsilon'' \quad (3)$$

Where, ε_0 is the vacuum permittivity and $\omega = 2\pi f$ with f being frequency.

3. Results and discussion

3.1 Phase and Surface Morphology

XRD Patterns of the proposed samples of the trivalent metal ion (Al^{+3}) doped $CoFe_2O_4$ system with basic chemical composition $CoAl_xFe_{2-x}O_4$ (here, x= 0.0, 0.1, 0.15, 0.2 and 0.25) are presented in Figure 1(a) and Fig 1(b). Presence of (220), (311), (400), (422), (511), (440) and (533) planes indexed for the cubic phase of spinel ferrites. All proposed nano-ferrite samples exhibited Fd-3m space group, which is confirmed by the JCPDS Card No: 22-1086 for the Al^{+3} doped $CoFe_2O_4$.

Microstructures were studied by placing the samples under Scanning electron microscope. Micrographs of the sintered samples are depicted in Fig. 2 (a-d), shows the surface structure for the proposed samples. All the samples are having well dispersed and dense structure.

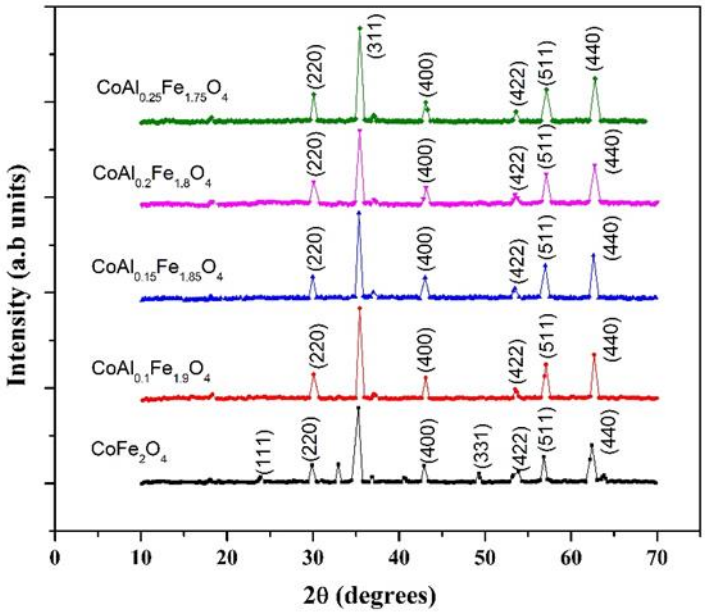

Fig.1. XRD Patterns of trivalent metal ion (Al^{+3}) substituted $CoFe_2O_4$

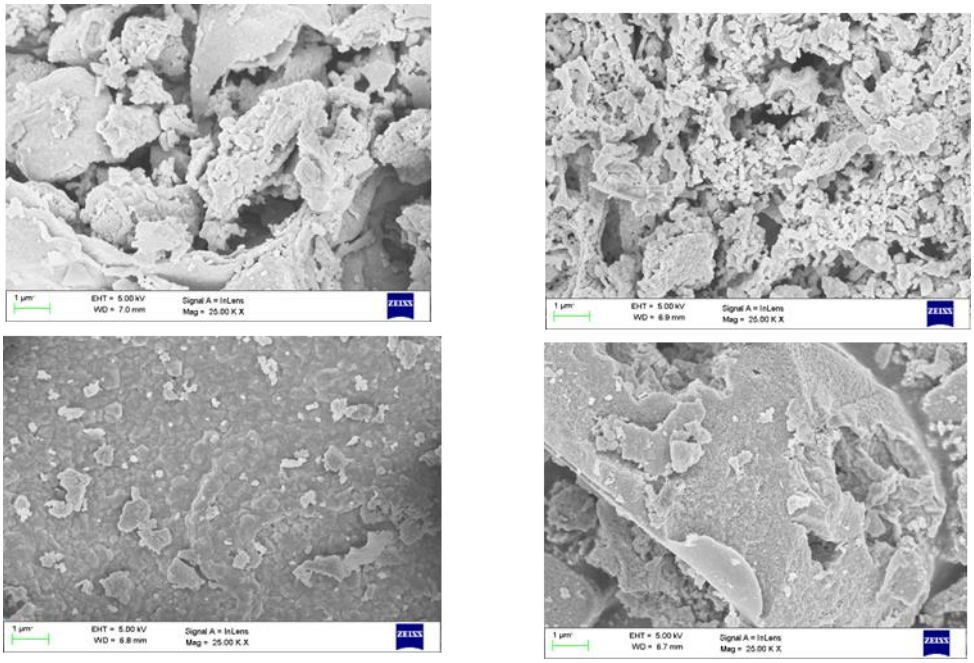

Fig. 2 Micrographs of Al^{+3} substituted (a) $CoAl_{0.1}Fe_{1.9}O_4$ (b) $CoAl_{0.15}Fe_{1.8}O_4$ (c) $CoAl_{0.2}Fe_{1.8}O_4$ (d) $CoAl_{0.25}Fe_{1.75}O_4$

3.2 Dielectric and Impedance Studies

Dielectric studies were carried out at RT to study the RLC behavior of the proposed samples in the frequency range from 100 Hz to 5 MHz Various dielectric parameters such as permittivity, ε' and ac conductivity (σ_{ac}) with respect to variation in frequency at room temperature for the synthesized samples is shown in Fig.3. From the Fig.3 (a), it is clear that ε' decreases with increasing frequencies and remains almost independent at higher frequencies. Variation of dielectric constant with applied frequency is due to charge transport relaxation. Dielectric dispersion is common in ceramics like ferrites and is attributed to Maxwell and Wagner type of interfacial polarization [14-15], as the dielectric constant is a combined effect of dipolar, electronic, ionic and interfacial polarizations. Since ionic polarization decreases with frequency, at higher frequency cycle rates, the constituent electric dipoles are unable to follow the quick variations of the alternating applied electric field and hence, measured ε' also decreased with frequency. Larger values of permittivity are related with space charge polarization at grain boundary and heterogeneous dielectric structure.

By electron exchange between Fe^{+2} and Fe^{+3}, displacement of electrons takes place with the applied field and these electrons determine polarization. Polarization decreases with increase in frequency and for further increase, the electric exchange between Fe^{+2}/Fe^{+3} cannot follow the alternating field hence reaches the constant value [16-17].

Variation in the dielectric loss for all the proposed series of samples upto the frequency range of 5 MHz at room temperature is shown in Fig. 3(d). Values of loss tangent (tanδ) represent the attenuation in these proposed ceramics and polarization being unable to respond to applied external frequency. Similar nature of curves for both ε' and tanδ are almost similar and may be correlated to the domain wall motion with the applied field, the electron exchange between Fe^{+2} and Fe^{+3} ions can correlate with the dielectric properties exhibited by proposed samples.

In order to understand the type of charge carriers and type of polarons responsible for conduction, ac conductivity, σ_{ac} were estimated as per $\sigma_{ac}= \omega \varepsilon_0 \varepsilon''$, with ε_0 is the permittivity of free space and $\omega=2\pi f$.

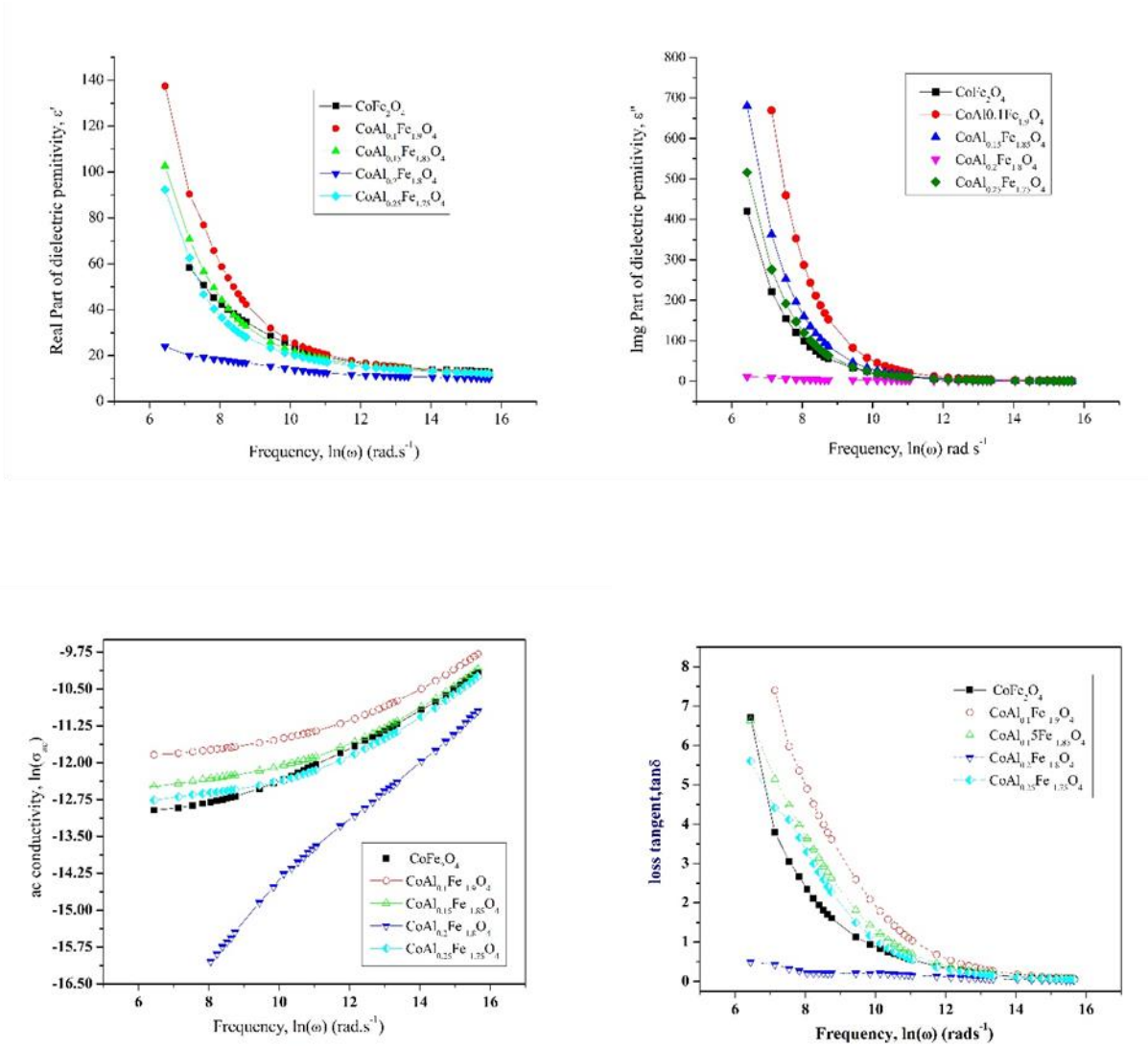

Fig.3 Variation of (a). Real Part of Dielectric permitivity, ε' with ln(ω) and (b) Imaginary Part of Dielectric permitivity, ε'' with ln(ω). (c) AC conductivity, ln (σ_{ac}) with ln(ω) and (d) Tangent loss factor tanδ with ln(ω).

For the synthesized samples, variation of a.c conductivity, σ_{ac} with frequency, ln (ω), is shown in Fig.3 (c). Obtained plots are almost linear for the entire range of frequency except at lower frequencies. Linear variation of σ_{ac} with frequency confirms that, conduction in mixed spinel ferrite occurs by the hopping of charge carriers between the localized states which confirms the small polaron type of conduction [18-20]. Conduction mechanism in spinel ferrites can be explained based on the hopping of charge carriers between Fe^{+2} and Fe^{+3} ions on octahedral lattice sites. Increase in the frequency of the applied field accelerates the hopping of charge carriers thereby enhancing the overall conduction process, thereby increasing the conductivity. At higher frequencies, ac conductivity (σ_{ac}), remains constant because the hopping frequency of the charge carriers no longer follows the external applied field variations and lags behind it. However, the decrease in conductivity values at lower frequencies can be correlated to conduction by mixed polarons.

Conclusions

Nano-powders of the system $CoAl_xFe_{2-x}O_4$ (here, x= 0.0, 0.1, 0.15, 0.2 and 0.25) were prepared successfully using auto-combustion method which involves nitrate-citrate precursors. Structural phase is confirmed

through XRD studies for the Al^{+3} substituted $CoFe_2O_4$ nano samples. Morphology of the nano-powders reveals the dense structures with well-defined grains. Finally, it is concluded that, trivalent metal ion (Al^{+3}) substituted $CoFe_2O_4$ nano-powders have been studied for structural and dielectric properties.

Acknowledgements
Authors are highly thankful to CENSE, IISc-Bangalore for providing PXRD and FESEM facilities to accomplish this research work.

References

1. R Ahmad, I.H Gul, M. Zarrar, H. Anwar, A. Khan, J. Magn.Magn.Mater ,405, pp.28 (2016).
2. R Zhang, L Sun, Z.Wang, W.Hao, E.Cao, Y.Zhang , Mater Res.Bull,98, pp.133 (2018).
3. R K Panda, R.Muduli, G.Jayarao, D.Sanyal, J.Alloys & Compd, 669, pp.19 (2016).
4. K K Bharathi, C V Ramana, Jour.Mater.Res ,26, pp.584-591 (2011).
5. H L Anderson, M Christensen, Nanoscale,7, pp.3481-3490 (2015).
6. R.Rani, G.Kumar, K.M Batoo, M.Singh , American Jour.Nanomater , 1, pp.09-12 (2013).
7. S.Darbagh A, A.Ati, S.K Ghoshal, S Zare., R M Rosnan, Z.Othaman, Bull.Mater.Sci,39, pp.1029-1037 (2016).
8. D D Andhare, Supriya R.P, J S Kounsalye, K M Jadhav, Physica B: Condensed Matter, 583,412051 (2020).
9. Geok B. Teh, David A. Jefferson, Jour. Solid State Chemistry ,167, pp.254-257 (2002).
10. S.Abdul Khader, Asiya Parveez, Arka Chaudhuri, M S Shekhawat and T.Sankarappa, Physica B: Condensed Matter, 584, May Issue, pp.411675 (2020).
11. S. Chikazumi, Physics of Magnetism, Chap.17, John.Wiley, New York, 1964.
12. Wagner KW (1913) Ann Phys 40:817.
13. Maxwell JC, Electricity & Magnetism, Vol 1, Oxford University Press, Oxford (1929).
14. Koops C G (1951) Phys Rev 83:121.
15. Ph.Tailhades, C.Villette, A.Rousset, G.U Kulkarni, K R Kannan and C N R Rao, Jour. Solid State Chemistry, 141, pp.56-63 (1998).
16. A. Gruskova, IEEE Trans Magn 30(2), pp.639-641 (1994).
17. Chikazumi S, Physics of Ferromagnetism, Oxford University Press, Oxford (1997).
18. G.H Jonker, Jour. Phys. Chem. Solids, Pergamon Press, Vol.9, pp.165-175 (1959).
19. Alberto E.Regazzoni , Egon Natijevic , Colloids and Surfaces , 6, pp.189-201 (1983).
20. Niu X, Du W and Du W, Sensors and Actuators B, 99 (2-3), pp.405-409 (2004).